Investigation into alternative testing methodologies for characterization of influenza virus vaccine

Tracy Tay*, Catherine Agius, Ross Hamilton, Jesse Bodle, and Steve Rockman

Influenza Research and Development; bioCSL Pty Ltd.; Parkville, Victoria, Australia

The objective of this study was to explore various testing methodologies suitable for characterizing sedimented or agglomerated material. To model this, bioCSL's split influenza virus vaccine, Fluvax® was utilized. The investigation was conducted on 5 dispensed lots of commercially manufactured vaccine, formulated for the 2013 Southern Hemisphere season. Vaccine syringes were initially inspected by visual tests; the material was then aseptically pooled for characterization assessment by microscopy and several agglomeration assays. All syringes passed bioCSL's description test where any fine or large sized particles of sediment observed in the vaccine were resuspended upon shaking; inverted light microscopy verified that the sediment morphology was consistent with influenza vaccine. Electron microscopic examination of pooled vaccine material demonstrated the presence of typical influenza structures including split virus, virosomes, whole virus particles and agglomerates. An optical density turbidity assay revealed relatively high protein recoveries in the vaccine supernatant post-centrifugation treatment, thus indicative of a well-dispersed vaccine formulation. This was corroborated by particle sizing analysis using dynamic light scattering which generated reproducible volume particle size distributions of a polydisperse nature. Ultraviolet-visible absorbance profiles further confirmed the presence of some agglomerated material. Data from all methods demonstrated consistent results between all batches of vaccine. Therefore, this investigation revealed the suitability and usefulness of the various methodologies in characterizing the appearance of agglomerated vaccine material. It is suggested that such methods may be applicable and beneficial for the development of a wider spectrum of heterogeneous and agglomerated formulations to provide safe, efficacious and superior quality biopharmaceutical products.

Introduction

Vaccination remains the cornerstone of preventing influenza, a highly contagious, acute, febrile respiratory disease caused by different influenza viruses. On a global scale, influenza epidemics result in 3 to 5 million cases of severe illness and up to half a million deaths per annum.[1]

Current seasonal influenza vaccines are trivalent or quadrivalent, containing purified and inactivated antigens against representative viruses of influenza A (H1N1 and H3N2 subtypes) and influenza B (from the Yamagata and/or Victoria lineages) predicted to circulate in the upcoming season each year. Two types of influenza vaccine are available, including an inactivated (killed) preparation administered via intramuscular injection, as well as a live attenuated, cold-adapted influenza vaccine delivered nasally. Inactivated vaccines are further categorized as whole virus, split virus or subunit types. Split virus and subunit vaccines are the most widely used influenza vaccines; they retain the

immunogenic properties of the viral proteins while exhibiting reduced reactogenicity particularly in infants and children compared to whole virus vaccines.[2,3]

Since the 1970s, the manufacture of inactivated trivalent influenza vaccine (TIV) has been largely based upon chemical disruption or "splitting" of the influenza virus.[4] Chemical disruption (by detergent or solvent) was found to reduce the reactogenicity of the vaccine without, in many cases, compromising the immunogenicity. The majority of currently available commercial influenza vaccines are disrupted or split with detergent due to the high volatility of solvents. Following splitting, further treatment is required to reduce the detergent to residual levels. As a consequence of reducing the detergent concentration the split virions develop agglomerates or agglomerated material due to hydrophobic interactions; this occurrence is in turn dependent on the strain and the level/type of detergent utilized in the splitting process.

Previous studies have demonstrated the formation of agglomerates in influenza vaccine formulations upon removal of the detergent. For example, subunit influenza vaccines exhibited mixed agglomerates when detergents including Nonidet-P40 and sodium dodecyl sulfate were removed from the preparation.[5] In addition, when nonionic detergents were used to solubilize glycoproteins of parainfluenza viruses and subsequently removed, agglomeration of proteins occurred due to hydrophobic bases that formed rosette-like clusters.[6]

The split virion influenza vaccine utilized as the model therapeutic agent in the current study is defined in the European Pharmacopoeia (EP) as an aqueous suspension comprising strains of influenza virus.[7] A common physical stability problem encountered with pharmaceutical suspensions is due to sedimentation, or the tendency for particles in suspension to settle out of the aqueous medium in which they are entrained to form a sediment at the bottom of the container.[8] The observation is that the flocs or agglomerates fall together to produce a distinct boundary between the sediment and supernatant liquid; the liquid above the sediment is clear because even the small particles present in the system are associated with the flocs. Therefore, in order to ensure uniform dosing of a stable suspension, the sediment must be able to be resuspended (i.e., readily dispersed) upon shaking.[9]

Protein agglomerates are common species that occur during different stages of manufacturing, formulation, storage, distribution and handling. Many protein-based pharmaceuticals exhibit a wide range of agglomeration phenomena. In order to gain a more profound understanding of the product quality attributes, it is important to be able to detect and monitor the occurrence of any agglomerated material. Furthermore, there is a crucial need within the biopharmaceutical industry to understand agglomeration pathways and the risk factors that can induce agglomeration from the beginning of the product development process, in order to align manufacturing processes with Quality by Design (QbD) principles. According to the Food and Drug Administration (FDA) Guidance for Industry for therapeutic protein products[10] and the Influenza Vaccines Quality Guideline provided by the European Medicines Agency,[11] it is recommended that either an individual or combination of methods should be utilized to characterize distinct agglomerated species in a product. However, currently there is no single analytical method which is able to accurately measure and characterize the full spectrum of particulate matter ranging from sub-visible ($<100~\mu m$) to larger agglomerates that may be present within the formulation. Characterization tools that improve detection, understanding and the progression of agglomeration would significantly facilitate troubleshooting, product development and process optimization.

This study aims to investigate an armory of testing methodologies suitable for characterizing a therapeutic agent that is comprised of multiple structural components, such as a split virion influenza vaccine, particularly in reference to sedimentation and agglomeration. Specific methods explored included tests by visual inspection, high-resolution microscopy, agglomeration assays and ultraviolet (UV)-visible absorbance spectroscopy.

Results

Visual inspection by description testing

Five lots of bioCSL's commercially manufactured inactivated influenza virus vaccine (IVV), Fluvax® for the 2013 Southern Hemisphere (SH) season were obtained for characterization testing (**Table 1**).

The results from the description test including additional comments for all 90 syringes across the 5 lots of IVV are shown in **Table 2**. Each syringe from all 5 lots passed the description test according to bioCSL's IVV description specification of "*clear to slightly opaque liquid containing some sediment which readily resuspends upon shaking.*" Furthermore, 84 of the total 90 syringes were identified to contain "*small amounts of fine sediment,*" and the remaining 6 syringes comprised "*large amounts and/or large sized particles of sediment,*" all of which "*resuspended upon shaking.*"

Inverted light microscopy analysis

Following the description test, 75 syringes from the 5 batches of 2013 SH dispensed vaccine were qualitatively tested by inverted light microscopy (ILM) in order to examine the morphology of any sediment present. In brief, the method involved capturing two ILM images of each syringe under the following conditions: (1) after leaving the syringes to lie sideways overnight at 2–8°C without shaking, then allowing to equilibrate to room temperature for a minimum of 30 min without shaking, and (2) after step 1 above, followed by vigorous shaking of the syringe for 20 times. Two representative ILM images from each lot of the IVV syringes captured under the above conditions are shown

Table 1. Details of examined lots of bioCSL's IVV for the 2013 SH season

Lot no.	No. of syringes
090634903	18
090635001	18
090636401	18
090637301	18
090638202	18

Table 2. Results of description test and additional comments for 5 lots of bioCSL's 2013 SH IVV (18 syringes per lot, 90 syringes in total)

IVV lot no.	Description test	Comments test
090634903	18 out of 18 PASS	All syringes were identified to contain *"small amounts of fine sediment observed in vaccine, all sediment resuspended upon shaking."*
090636401	18 out of 18 PASS	
090638202	18 out of 18 PASS	
090637301	18 out of 18 PASS	From each lot, 15 syringes were identified to contain *"small amounts of fine sediment"* and the remaining 3 syringes comprised *"large amounts and/or large sized particles of sediment,"* all of which *"resuspended upon shaking."*
090635001	18 out of 18 PASS	

in **Figure 1** and the results summarized in **Table 3** (where *US* and *S* denote syringes that were unshaken and shaken, respectively).

From the ILM results presented in **Figure 1** and **Table 3** for each of the 75 syringes across the 5 lots of dispensed IVV, a sediment morphology which was "*consistent with influenza vaccine*" was recorded, both prior to and after shaking of the syringes. This result was confirmed by electron microscopy (EM) analysis and will be discussed in further detail in the following section. The ILM images depicted the presence of sediments of small and large particles, which are typically found in influenza vaccine. Interesting to note however, is that for all the images captured after shaking of the syringes, a reduction in sediment formation is apparent (**Fig. 1**). This observation indicates that any sediment present can be resuspended or readily dispersed upon shaking.[9]

Material from the 75 syringes across the 5 IVV batches was then aseptically pooled to obtain a total of 25 pooled samples (5 pooled groups per batch) for subsequent EM, optical density turbidity (ODT) and dynamic light scattering (DLS) analyses. The results from each of these assays are described below.

Electron microscopy analysis

Imaging by EM was used to assess the appearance of the pooled IVV samples. For each of the 5 lots of pooled 2013 SH IVV, EM photographs were taken at both low and high magnifications (i.e., at 32,200× and 108,500×, respectively). Representative EM images from each lot of IVV material are presented in **Figure 2** below.

Typical influenza viruses are identified by the presence of evenly distributed (antigenic) spikes of the glycoproteins hemagglutinin (HA) and neuraminidase (NA), which coat the entire viral envelope.[12] The EM images (taken at a magnification of 108,500×) across all 5 lots of 2013 SH IVV were observed to contain structures consistent with that of influenza virus (**Fig. 2A–E**). Specifically, the structures identified in the EM images included rosettes and caterpillars (sections of the split
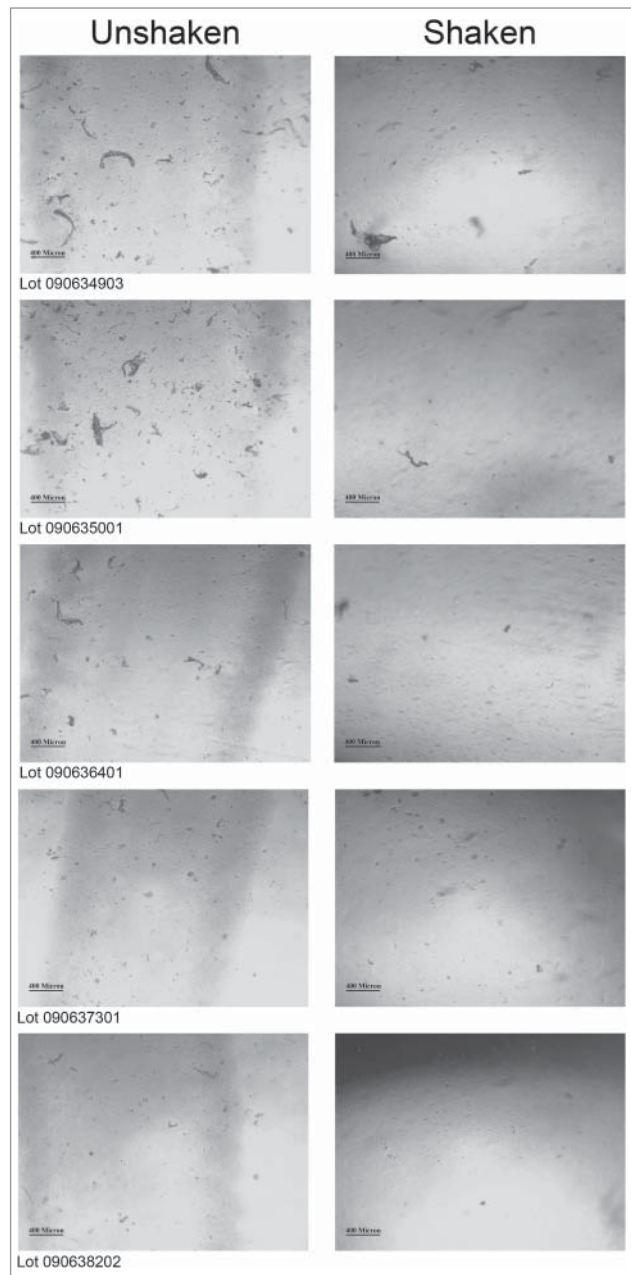
Figure 1. Representative ILM images for 5 lots of bioCSL's 2013 SH IVV, including lots 090634903, 090635001, 090636401, 090637301 and 090638202, when syringes were left unshaken (left column) and following vigorous shaking (right column).

virus membrane embedded with antigenic spikes of HA and NA that are folded into various shapes), virosomes (spherical, unilamellar vesicles with an empty influenza virus envelope that is devoid of internal proteins and genetic material of the virus), membranes, slightly disrupted virions and whole virions (intact influenza structures comprising genetic material encased by a membrane of HA and NA spikes, immediately prior to being split or disrupted). Predominant structures were comprised of split influenza virus.
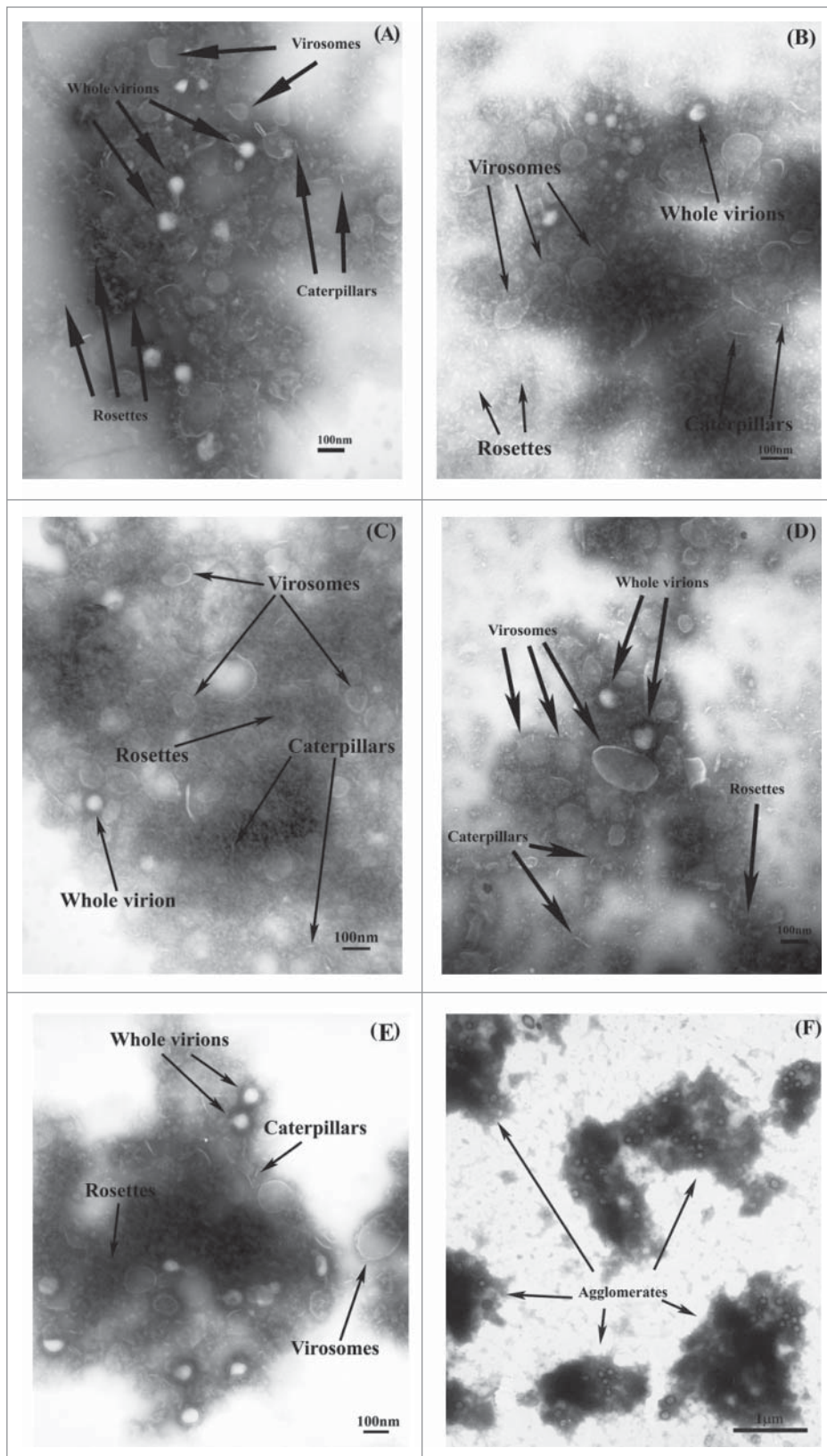
Figure 2. Representative EM images for pooled material corresponding to each of the 5 lots of bioCSL's 2013 SH IVV at a magnification of 108,500x for lots (**A**) 090634903, (**B**) 090635001, (**C**) 090636401, (**D**) 090637301 and (**E**) 090638202; and at a magnification of 32,200x for lot (**F**) 090638202.

EM analysis was also performed on the samples at a lower magnification (32,200×) in which observations were consistent across all 5 batches of IVV; a representative image from one of the lots is shown in **Figure 2F** below, depicting agglomerates of split influenza species represented by the darker regions of the micrograph.

Agglomeration assessment by the optical density turbidity assay

To monitor the extent of agglomeration, the ODT assay was used to measure the recovery of protein in the supernatant of IVV material after application of a moderate relative centrifugal force (RCF) of 13,684 g for 1 min. Several attributes of the ODT assay were examined for IVV material, including repeatability (CV = 5.7%), inter-lot precision (CV = 7.2%) intermediate precision (CV = 4.5%), assay response to agglomerate dissociation (R^2 = 0.990; p = 0.01 significant slope) and linearity (R^2 = 0.955; p = 5.6×10^{-6} significant slope) (data not shown).

Figure 3 presents an ODT plot summarizing the average protein recovered in the supernatant of the 25 pooled samples across the 5 batches of IVV material (expressed as %ODT). The results indicated consistent inter-lot supernatant recoveries in the range of 54.6 to 63.3%, suggesting a relatively well-dispersed vaccine formulation. These values were in close agreement with the mean results obtained from the ODT validation study (performed on 2013 SH IVV) for repeatability (56.9 ± 3.3%), inter-lot variability (55.1 ± 4.0%) and intermediate precision (57.2 ± 2.6%). Hence, the current analysis further substantiated the ODT assay as a robust and accurate method for characterizing the agglomeration state of the material examined.

Particle sizing by dynamic light scattering

DLS was used as a complementary method to analyze and characterize agglomeration and to determine the validity of the ODT assay. For accurate DLS measurements, the density,

Table 3. Summary of ILM results for the appearance of bioCSL's 2013 SH IVV

Lot no.	No. of syringes	Unshaken (US) / Shaken (S)	Observations: morphology of sediment, if present, is consistent with that of influenza vaccine?
090634903	15	US	YES
		S	YES
090635001	15	US	YES
		S	YES
090636401	15	US	YES
		S	YES
090637301	15	US	YES
		S	YES
090638202	15	US	YES
		S	YES

Table 4. Density, viscosity and refractive index (RI) properties of pooled 2013 SH IVV for DLS analysis at 25°C

	Pooled 2013 SH IVV
Density (g/cm^3)	1.003
Viscosity (cP)	0.923
RI	1.3342

viscosity and refractive index (RI) of a representative pooled IVV sample were pre-determined at a temperature of 25°C and included in the measurement protocol of the Zetasizer software (**Table 4**).

From each DLS measurement, a particle size distribution (PSD) based on intensity is obtained, which demonstrates the relative intensity of light scattered by particles in various size populations. For each of the 5 batches of 2013 SH IVV, the average intensity PSDs revealed reproducible profiles of a polydisperse nature (**Fig. 4**), i.e., 2 distinct size populations were present in the samples post-centrifugation treatment, including a monomodal peak at 150 nm and a shoulder peak at 5500 nm.

In order to more accurately represent the data, the intensity PSDs for each of the 5 pooled samples within each batch of IVV were then converted using Mie[13] theory to volume PSDs; these
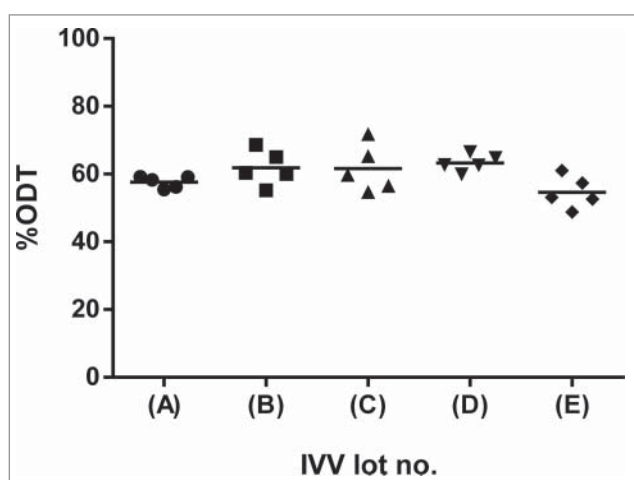
Figure 3. Average protein recovery in supernatant (expressed as %ODT) for 5 pooled groups within each of 5 lots of bioCSL's 2013 SH IVV, including lots (**A**) 090634903, (**B**) 090635001, (**C**) 090636401, (**D**) 090637301 and (**E**) 090638202, by ODT analysis post-centrifugation at an RCF of 13,684 g for 1 min.

distributions describe the relative proportion of each size class inherent to the sample based on particle volume. The profiles that were generated remained bimodal however a slight shift in the distributions to smaller particle sizes was apparent (**Fig. 5**), i.e., the corresponding monomodal peak is shown at 90 nm and the shoulder peak at 4800 nm. The greater relative proportion of particles present in the smaller size population of the volume PSDs along with the reproducible profiles across the 5 lots of IVV suggested a homogeneous vaccine formulation with minimal agglomeration occurring within the samples. Furthermore, statistical analysis performed using one-way analysis of variance (ANOVA) indicated no significant differences between the 5 lots of IVV with respect to the mean volume PSDs ($P > 0.05$ each). The consistent PSDs corroborated the ODT data where the proportion of dispersed material was also comparable across the 5 lots of IVV.

Agglomeration assessment by UV-visible absorbance spectroscopy

The caveat of using DLS is the requirement of a preparatory centrifugation step that may have removed larger particles and subsequently resulted in the more distinct monomodal appearance of IVV. Hence to confirm the agglomeration assessment by DLS, an additional UV-visible absorbance spectroscopy method was employed which excluded the pre-centrifugation treatment of samples. This is a turbidimetric method which monitors protein agglomeration by measuring the optical density (OD) of the sample based on light scattering in the near UV or visible region, where proteins exhibit negligible absorption.

For each lot of IVV, UV-visible absorbance analysis was performed neat and in triplicate, i.e., on three separate syringes. The final average plots of absorbance versus wavelength for the 5 lots of IVV (**Fig. 6**) were generated by subtracting the Vaccine Diluent control data from those of each syringe sample. These results provide informative agglomeration data based on both the protein concentration as well as agglomeration levels defined by an agglomeration index (AI), which will be discussed in further detail below.

Firstly, it is well known that one of the factors affecting agglomeration is the protein concentration; increasing protein concentration during refolding usually increases protein agglomeration due to the increased propensity of intermolecular interactions.[14,15] Simulation of *in vitro* protein refolding and agglomeration indicates that agglomeration dominates over refolding at high protein concentrations and the size of protein agglomerates increases proportionally with protein concentration.[16] By measuring the absorbance

arising from the intrinsic chromophores (tryptophan, tyrosine and cysteine) in the protein solution, the protein concentration can then be determined by its directly proportional relationship, according to Beer-Lambert's Law:[17]

$$c = \frac{A}{\varepsilon l} \qquad \text{Equation 1}$$

Where c is the molar concentration (mol L^{-1}), l is the optical pathlength (cm), ε is the molar extinction coefficient (L mol^{-1} cm^{-1}) and A is the absorbance at a given wavelength.

In a preliminary investigation, analysis by the UV-visible absorbance assay enabled an understanding of the agglomeration behavior within intermediate influenza vaccine material. For example, a substantial increase in absorbance due to light scatter was evidenced during the process at which inactivated virus material was produced into intermediate vaccine material; this correlated well with the formation of agglomerates, as increasing concentrations of detergent was removed. In addition, a time course study was conducted on supernatants of intermediate vaccine material for A/Victoria/210/2009, A/California/7/2009 and B/Brisbane/60/2008 influenza virus strains, whereby the degree of agglomeration was monitored over a period of 9 weeks by the UV-visible assay. The results demonstrated higher absorbance values for all samples at 9 weeks compared to the initial time point; this was attributed to increased amounts of agglomerates over time that were not removed by centrifugation treatment.

In the current study, consistent and reproducible UV absorbance profiles showed positive absorbance readings in the wavelength region of 250–300 nm (**Fig. 6**). Comparison of the mean UV absorbance data using one-way ANOVA did not demonstrate any significant differences between the profiles of the 5 IVV lots ($P > 0.05$ each). Hence this demonstrated that the corresponding level of agglomeration did not vary statistically between all 5 lots of the IVV samples.

Secondly, an additional parameter that is commonly used to correct for turbidity (i.e., light scattering) effects is the agglomeration index (AI) defined by the following equation:

$$AI = \frac{A_{350}}{(A_{280} - A_{350})} \times 100$$

$$\text{Equation 2}$$

Where A_{280} and A_{350} are the measured absorbance values at wavelengths of 280 and 350 nm, respectively. The AI parameter not only measures the OD$_{350}$ but also corrects for protein content, i.e., the absorbance of proteins at 280 nm.[18] Hence, an increase in OD signals in the non-absorbing region of a protein's UV spectrum (>320 nm) is considered indicative of agglomeration occurring within the sample, i.e., agglomeration increases proportionally with the AI parameter.

The calculated AI values shown in **Table 5** were comparable across the 5 lots of 2013 SH IVV and ranged between 45.6 and 49.6% ($P > 0.05$ between each lot of IVV; one-way ANOVA), hence indicating consistent levels of agglomeration with minimal variation. The consistency of these results by UV analysis where samples were tested neat additionally confirmed the observations by DLS, despite the removal of any extraneous or sedimented material due to the pre-centrifugation step applied in the latter approach.
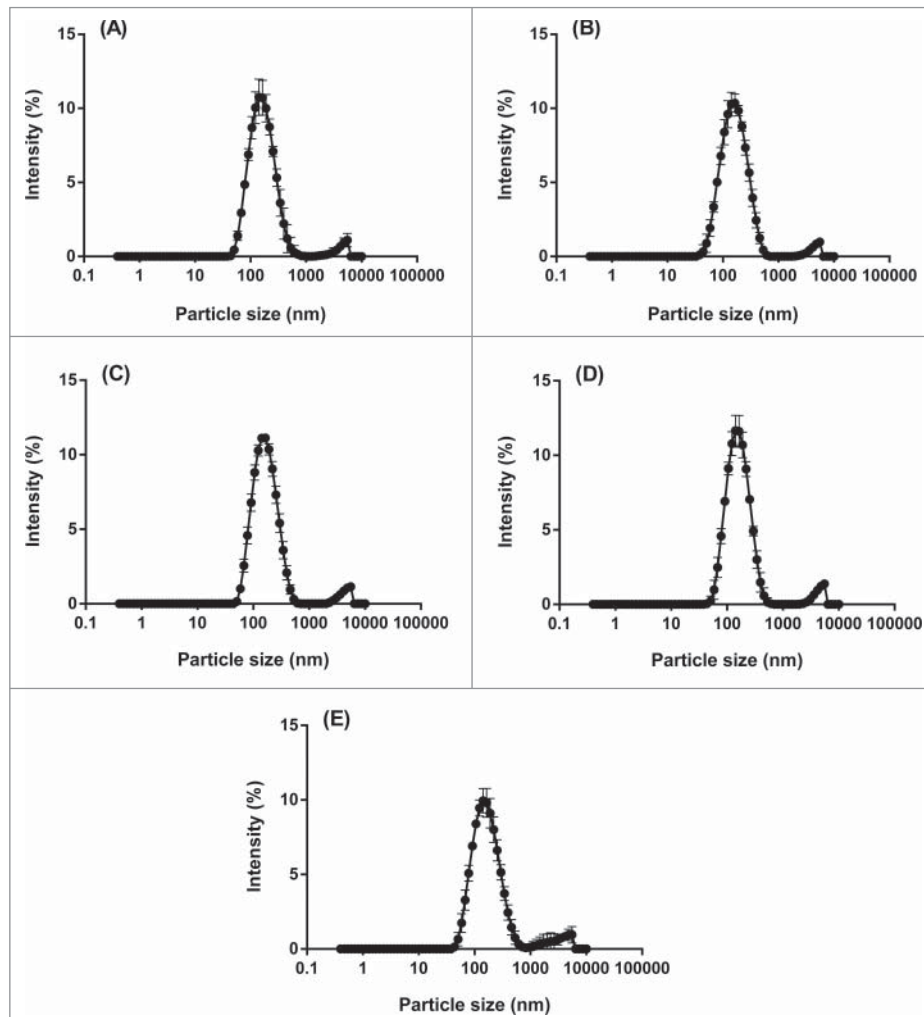
Figure 4. Average intensity PSDs (n = 5) of the supernatant for 5 pooled groups within each of 5 lots of bioCSL's 2013 SH IVV, including lots (**A**) 090634903, (**B**) 090635001, (**C**) 090636401, (**D**) 090637301 and (**E**) 090638202, by DLS analysis at 25°C post-centrifugation at an RCF of 6,082 g for 1 min.

Discussion

The analysis of complex pharmaceuticals that contain a multitude of particle types including agglomerated material is challenging. At this time there is no single instrument or method that can adequately cover the entire spectrum of agglomerate sizes (ranging from submicron to visible), types and structures. Therefore, a variety of biophysical methods must be used to detect and characterize protein agglomerates that exist in biopharmaceutical products. A discussion on some commonly used methods which have been attempted for agglomerate measurement and characterization is provided below.

Size exclusion chromatography (SEC) is the most widely used tool for agglomerate characterization as it is a sensitive, high throughput, relatively inexpensive and a simple method to implement.[19] The technique is based on proteins and their agglomerated complexes that separate with differing extents of permeation into the pores of a stationary phase (e.g. silica-based polymeric beads).[20] Larger molecules or agglomerates are excluded from the resin pores and therefore elute rapidly, while smaller molecules with greater access to the pores elute more slowly. However, the SEC can only separate agglomerates over a limited size range and has poor resolution for larger soluble agglomerates that may be eluted out at the void volume. Insoluble agglomerates are also often filtered out by the column matrix and therefore not captured by the detectors. For these reasons SEC was not applied to the vaccine samples in the current work. SEC requires complementary cross-validation using orthogonal techniques such as analytical ultracentrifugation (AUC), field flow fractionation (FFF) or light scattering.

AUC and FFF are methods which provide resolution of agglomerates or particles ranging from 0.001 to 50 μm in size.[21] In addition, both methods are able to accurately estimate the quantity, size and shape of multiple protein agglomerate species without the use of molecular weight standards.[22-24] However, these methods are limited by their ability to detect low levels of protein agglomerates, and further require highly trained and specialized personnel for instrumentation operation and data analysis. AUC has played an important role since the early days of the biotechnology industry, such as for the purposes of characterizing the association-dissociation of insulin hexamers[25] and recombinant insulin mutants engineered to alter the association and
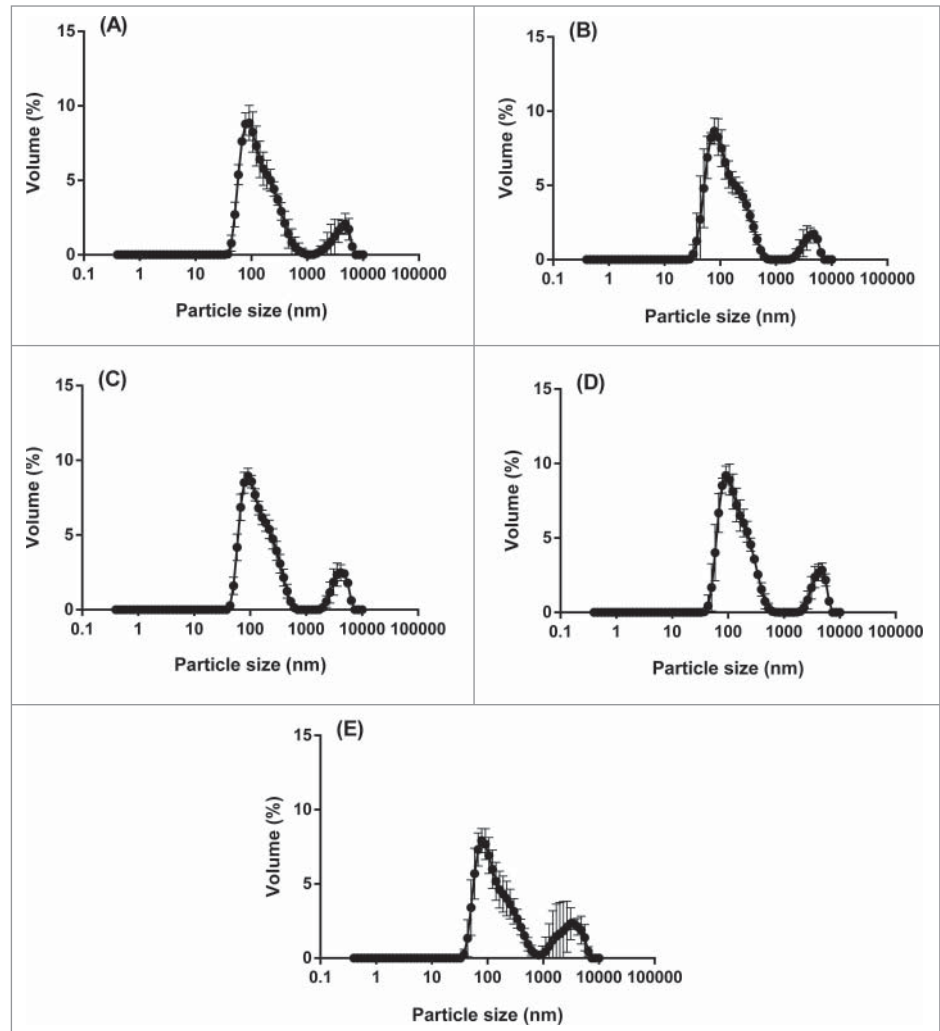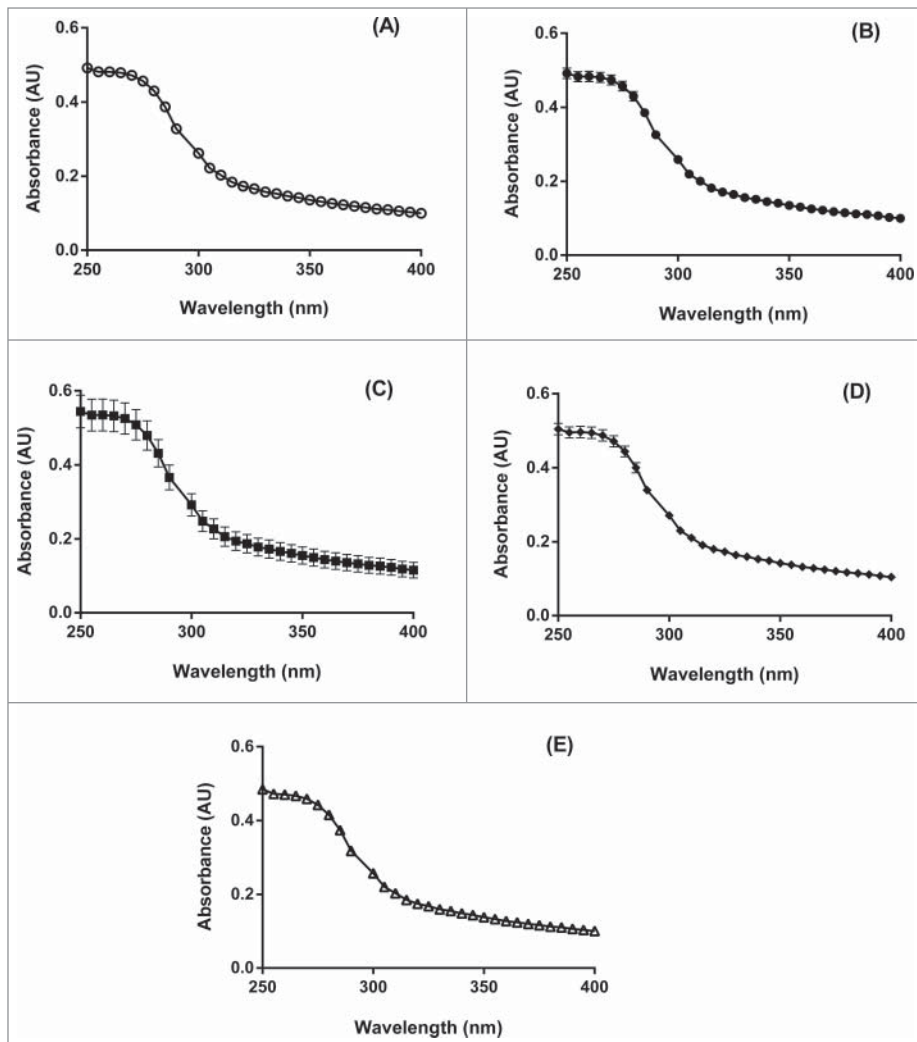

Figure 5. Average volume PSDs (n = 5) of the supernatant for 5 pooled groups within each of 5 lots of bioCSL's 2013 SH IVV, including lots (**A**) 090634903, (**B**) 090635001, (**C**) 090636401, (**D**) 090637301 and (**E**) 090638202, by DLS analysis at 25°C post-centrifugation at an RCF of 6,082 g for 1 min.

hence bioactivity.[26] For most biotechnology applications, the AUC method is typically based on the physical principles of sedimentation velocity; this involves spinning the sample (with a high speed centrifuge at speeds of up to 60,000 rpm) and an optical system that measures the rate at which the different components sediment to form a pellet.

FFF is a flow-based separation technique that separates macromolecules based on their differences of diffusion coefficients.[27] The retention and separation of samples are controlled by an external field, perpendicular to channel flow. The FFF method is best suited for analyzing larger agglomerates that can be easily filtered by a SEC column matrix or sediment under centrifugal field. Several successful applications of FFF have been previously reported in the separation of protein agglomerates and other large biomolecules.[28,29]

Light scattering is a robust method and is used to monitor variation in the size of proteins due to conformational changes. This form of analysis is categorized as either static light scattering

Figure 6. Average UV-visible absorbance (AU) vs. wavelength (nm) profiles for 5 lots of bioCSL's 2013 SH IVV, including lots (**A**) 090634903, (**B**) 090635001, (**C**) 090636401, (**D**) 090637301 and (**E**) 090638202, performed neat for each lot (n = 3).

a tendency to overestimate the width of the peaks in the distribution; this effect is magnified when the fundamental intensity distributions are transformed to either number or volume distributions. For this reason, number and volume PSDs should only be used for comparative purposes, or for estimating the relative proportions where there are multiple peaks.[31] On the other hand, the intensity PSD can be used to accurately report the size of each peak in the distribution.

Despite the widespread use of the above methods, their applications have been limited to purified protein preparations such as immunoglobulins, antibodies, recombinant proteins and coagulation factors but not virus-derived vaccine antigens. Hence, analysis of agglomerates within more complex, pleomorphic and heterogeneous protein material would require the use of alternative methodologies. As there is no single instrument that encompasses the entire measurement range from sub-visible to agglomerated material within a formulation and each of the techniques used herein to characterize the complex nature of proteins will have its own limitations, combining multiple technologies offers a holistic overview and more profound understanding of the product. In the current investigation, a range of techniques was explored on a model complex biopharmaceutical agent, namely bioCSL's split virion influenza vaccine.

Results obtained from the description test indicated that all syringes satisfied the description criteria based on the EP specifications for product appearance and stability. This included the requirement for the vaccine to be a clear to slightly opaque liquid, as well as any sediment present within the vaccine to readily resuspend upon shaking.

While visual inspection of the syringes satisfied description testing criteria, this test relies on the subjective analysis of syringe contents by each operator and the reproducibility of syringe shaking performed by hand to resuspend any sediment present. However, adoption of a correlative microscopy approach which combines the use of both light and electron microscopy techniques (i.e., ILM and EM) allows a more comprehensive analysis of the IVV samples. The use of these 2 complementary methods yields a broader range of information regarding the overall vaccine presentation as well as the more intricate structural details of the constituents at a subviral level. In contrast to description testing, the visual appearance of IVV material is documented by ILM and EM analyses through the images that are captured.

(SLS), which measures the intensity of scattered light as a function of angular dispersion, or dynamic light scattering (DLS), where the diffusion rate of protein particles in solution is determined.[30] The main distinction between the 2 techniques is that SLS detectors measure molecular mass independently of molecular shape, whereas DLS detectors measure hydrodynamic size which depends on both mass and shape. The DLS technique has

Table 5. Agglomeration index (AI;%) for 5 lots of 2013 SH IVV, determined from UV-visible absorbance spectroscopy analysis

2013 SH IVV Lot no.	Average A_{280}	Average A_{350}	AI (%)
090634903	0.430	0.136	46.2
090635001	0.430	0.135	45.6
090636401	0.479	0.155	47.6
090637301	0.444	0.142	46.9
090638202	0.415	0.138	49.6

This therefore enables the visual appearance of the samples to be either referenced or reviewed at a later date.

Using the first microscopic technique by ILM, an overall examination of the IVV is performed in its native state by capturing images through the syringe, i.e., the material is not removed from the syringe for analysis. Thus, ILM is a low resolution technique and was employed in this study for the purposes of assessing whether any sediment present could be easily resuspended upon agitation. For each lot of IVV that was examined, the results demonstrated an apparent reduction in sediment formation in syringes after shaking hence suggestive of a physically stable vaccine formulation.

Subsequent to ILM analysis, pooled IVV material from the syringes were applied onto a grid for direct examination by EM. This higher resolution technique allows for a more detailed insight into the specific particle types present and their associated structural and morphological properties. EM analysis revealed that the constituents within the syringes were typical influenza virus structures and more importantly, verified that the vaccine predominantly consisted of split influenza virus in accordance with the requirements outlined by the EP for suspensions for injections.[7,9] Thus, alongside description testing, the complementary assessment by both ILM and EM provides a robust analysis of the appearance and nature of the viral structures, sediments and agglomerates within IVV material.

Use of the DLS technique provided information relating to the overall size distribution profile of particles within IVV. Furthermore, the analysis proved purposeful in revealing the consistent homogeneity of the material with minimal agglomeration occurring; however, caution must be exercised during interpretation of the results since a pre-treatment step was applied to remove any extraneous material that may interfere with the measurements.

As a means to overcome this caveat, UV-visible absorbance spectroscopy was performed on neat IVV material and the subsequent analysis confirmed the agglomeration assessment by DLS. Of all the techniques, the use of a turbidimetric method, namely the ODT assay, was found to be the most suitable in quantifying the level of agglomeration occurring within IVV material. The assay itself requires less than 3 minutes per sample to perform and minimal reagents and equipment are needed. The results indicated consistent protein recoveries in the supernatant, which corroborated well with the DLS and UV-visible data hence suggesting a relatively well-dispersed vaccine formulation. This has been further substantiated from previous analysis of intermediate influenza vaccine material that produced consistent and reproducible results over an extended period of time (data not shown).

Any previous attempts at assessing the product quality attributes have required a multitude of biophysical methods to characterize and measure agglomeration within a complex biopharmaceutical agent such as the split virion influenza vaccine. This is because no single instrument or technique is able to sufficiently encompass the varied sizes and types of agglomerates present. Hence, the novel and innovative use of the combined methods explored in this investigation could be applied to advance the formulation development of heterogeneous and agglomerated biopharmaceutical products.

This study was focused on assessing one particular aspect of the vaccine product, namely the agglomeration characteristics. In future work, it may be useful to correlate these outcomes to other attributes of the vaccine, such as potency, virus splitting profile, sterility and/or total protein.

Materials and Methods

Materials

Five lots of bioCSL's commercially manufactured inactivated IVV, Fluvax® for the 2013 SH season were obtained for characterization testing (18 syringes per lot, 90 syringes in total), as detailed in **Table 1**. All lots were dispensed at Parkville, Victoria, Australia and within specified expiration dates when analyzed.

The 2013 SH IVV formulation included the following influenza strains:

- H1N1: A/California/7/2009
- H3N2: A/Victoria/361/2011
- B: B/Hubei-Wujiagang/158/2009

Methods

A range of characterization tests was performed on the material within all IVV syringes. In summary, each syringe was initially inspected for description with additional comments (using bioCSL's description test for IVV), and examined by ILM; the IVV material within the syringes was then aseptically pooled in a sterile, particle free container for subsequent analysis by higher resolution EM, and 2 agglomeration assays based on the OD of influenza virus protein sedimentation (ODT assay) and particle sizing analysis (DLS). UV-visible absorbance spectroscopy was also utilized to gain an understanding of the agglomeration behavior. The following subsections will detail each of the methodologies used in this study.

Description test

For each of the 5 lots of IVV, the individual syringes were numbered and the age at the time of testing noted. Each syringe was inspected in accordance with bioCSL's currently Therapeutic Goods Administration (TGA) registered description test for product release and stability assessment of dispensed IVV, as summarized below.

As stated on the Product Information document,[32] bioCSL's Fluvax® is an inactivated influenza vaccine (split virion) suspension for injection, and is further described as *"a clear to slightly opaque liquid with some sediment that resuspends upon shaking."* This description is based on the requirements outlined in the EP which indicates that the *"vaccine is a slightly opalescent liquid"* and that *"suspensions for injection may show a sediment which is readily dispersed on shaking to give a suspension which remains sufficiently stable to enable the correct dose to be withdrawn".*[9]

The material in the syringes was examined and described in terms of color, clarity (degree of opalescence), viscosity and

settling behavior. The sample was observed by both reflected and transmitted light and against light and dark backgrounds. The presence of particulate matter, foreign material or agglomeration of particulate material was also noted.

Each syringe was assessed as a PASS/FAIL against the following specification: *"clear to slightly opaque liquid containing some sediment which readily resuspends on shaking."* Resuspension of the material within the syringes was achieved by vigorous shaking performed by hand, end to end from 10 to 20 cm, for 20 times in approximately 7 seconds. Additional comments to supplement the description test involved noting the appearance of each syringe as either:

- No sediment observed in the vaccine (PASS);
- Small amounts of fine sediment observed in vaccine, all sediment resuspended upon shaking (PASS);
- Large amounts and/or large sized particles of sediment present in vaccine, all sediment resuspended upon shaking (PASS);
- Sediment present in vaccine, not all sediment resuspended upon shaking (FAIL);
- Vaccine of atypical appearance, discoloration observed (FAIL); or
- Vaccine of atypical appearance, foreign object observed (FAIL)

Inverted light microscopy

Following description testing, the syringes were analyzed by ILM (Carl Zeiss AG, Jena, Germany) as a qualitative test to verify whether the morphology of any sediment present was consistent with that of influenza vaccine. Analysis was performed on the syringes at room temperature, both before and after shaking as detailed below.

Prior to examination, the syringes were stored at 2–8°C and placed lying sideways overnight without shaking. The first light micrograph was captured after allowing the syringes to equilibrate to room temperature for at least 30 min (no shaking). Each syringe was then shaken vigorously for 20 times as per the description test method described for resuspended IVV; the second light micrograph was then taken (after shaking). A brief description was also recorded for each image captured.

Pooling of samples

In order to obtain adequate sample volume for further characterization testing, it was necessary to pool the material from the 5 batches of IVV. Material from 15 syringes comprising each IVV batch was aseptically pooled into 5 separate groups (i.e., in lots of 3 syringes). This amounted to a total of 25 pooled samples across the 5 batches of IVV for subsequent analysis by EM, ODT and DLS.

Electron microscopy

Imaging of the pooled IVV samples was performed using a CM-10 transmission electron microscope (TEM) (FEI Company, Eindhoven, The Netherlands), operated at 100 kV. This form of microscopy (EM) provides images at higher resolution and magnification than is otherwise achievable with a light microscope (ILM). Specifically, negative stain EM was used as a simple qualitative method to assess the:

- presence/absence of whole virions
- presence/absence of agglomerated influenza and if present, a description of the shape and form
- presence of typical or atypical influenza structures

The agar diffusion filtration method developed by Hayat and Miller[33] was adopted for the current analysis. Three grids of each sample were prepared; the sample (1 μl) was applied neat to a formvar-coated copper electron microscope grid, which was then inverted onto a 2%w/v agar plate. Upon settling of the grids onto the agar plate (i.e., the liquid absorbed by the agar), the grid was floated on a drop of negative stain (2%w/v sodium phosphotungstate at pH 7.0). After twenty seconds, the grid was then lifted and excess stain removed by contacting the edge of the grid with a small strip of torn Whatman No. 1 filter paper. The remaining thin film of stain was left to air-dry prior to examination by the TEM at magnifications of 32,200 and 108,500×.

Optical density turbidity assay

To evaluate the degree of non-agglomerated material in the formulated IVV, the level of recovered protein was determined utilizing OD at A_{280} of the supernatant following the application of a moderate RCF. Since the proportion of protein in the pellet after centrifugation directly correlates to the degree of high density agglomerated material within the sample, a greater recovery in the supernatant would correspond to an increased proportion of dispersed protein.

The NanoDrop ND-1000 UV-visible spectrophotometer (Thermo Fisher Scientific, Wilmington, USA) was used to conduct OD measurements at a wavelength of 280 nm (i.e., A_{280}). A blank reading was initially taken by applying 2 μl of phosphate buffered saline onto the measurement pedestal and the pedestal then cleaned with a lint-free wipe after blanking. The IVV sample was vortexed briefly before adding 2 μl onto the pedestal and duplicate readings (A_{280}) of the neat sample obtained. Sample aliquots of 100 μl were then transferred into each of 2 fresh 1.5 ml microfuge tubes (Eppendorf, Hamburg, Germany) and centrifuged at an RCF of 13,684 g for 1 min in a Biofuge pico Heraeus benchtop microcentrifuge (Kendro Laboratory Products, Newtown, Connecticut, USA); duplicate readings of the supernatant post-centrifugation for each of the 2 replicate samples were measured and recorded. The average recovery of protein in the supernatant was determined from the protein concentration ratio of the supernatant relative to that of the neat IVV sample, using the mean values from each of the duplicate readings. Final protein recovery values were reported as %ODT (ranging from 0 to 100%), which increase with the amount of low density agglomerated protein in the sample. Refer to **Table 6** which provides an example analysis for determining the final protein recovery of a sample (%ODT) using the ODT assay.

Dynamic light scattering

Particle size analysis by DLS was used as a complementary method to the ODT assay to further understand the characteristics of agglomerated material within the samples. The DLS technique is based on measuring the Brownian motion of proteins in

Table 6. Example ODT analysis for IVV

	Initial A_{280} (mg/ml) [A]	Supernatant post-centrifugation A_{280} (Sample 1) (mg/ml) [B]	Supernatant post-centrifugation A_{280} (Sample 2) (mg/ml) [C]	% Recovery (Sample 1) [D]	% Recovery (Sample 2) [E]	Average % Recovery [F]	Standard Deviation (stdev) of % Recovery ($\pm$)
Description of analysis	A_{280} of neat sample (2 replicates)	A_{280} of supernatant after centrifugation (2 replicates)	A_{280} of supernatant after centrifugation (2 replicates)	$= B / A * 100$	$= C / A * 100$	$= (D + E) / 2 * 100$	$= $ stdev (D and E)
Example IVV	Avg A_{280} (0.61, 0.59) $= 0.60$	Avg A_{280} (0.36, 0.35) $= 0.36$	Avg A_{280} (0.36, 0.33) $= 0.35$	59.2	57.5	58.3	1.18

solution, which is the random movement of particles due to collisions with the surrounding solvent molecules. The Brownian motion induces time dependent fluctuations in the intensity of scattered light which is measured by DLS and subsequently generates an intensity PSD for the sample.

DLS measurements of the samples were performed using the Malvern Zetasizer Nano Series ZS (Malvern Instruments Ltd, Worcestershire, UK). Several properties which influence the Brownian motion of particles in solution were pre-determined for a representative pooled IVV sample, including the density (DA-100M Density Meter; Mettler Toledo, Columbus, Ohio, USA), viscosity (Lovis 2000M rolling-ball viscometer; Anton Paar, Graz, Österreich, Austria) and RI (30GS Refractometer; Mettler Toledo, Columbus, Ohio, USA). Pre-treatment of samples involved centrifugation for 1 minute at an RCF of 6,082 g (Biofuge pico Heraeus benchtop microcentrifuge; Kendro Laboratory Products) to remove any extraneous material or sediment containing large particles which are unstable and subsequently interfere with the analysis. The resulting supernatant component of each sample was then withdrawn and assessed by DLS; each sample measurement was based on 5 replicates (n = 5) performed at a backscatter angle of 173° and equilibrated to a temperature of 25°C for 3 minutes.

UV-visible absorbance spectroscopy
UV-visible absorbance spectroscopy was employed to further characterize the appearance of IVV material. This technique measures the degree of light scattering due to the association of proteins, for example oligomerization and agglomeration.[34] Thus, an increase in OD signal in the non-absorbing region of a protein's UV spectrum (>320 nm) would be indicative of agglomeration occurring. The analysis was performed neat and in triplicate, i.e., using three syringes for each of the 5 lots of IVV that were previously assessed by the description test.

The method involved removing the required number of syringes from storage at 2–8°C and allowing them to equilibrate to room temperature (23°C) for 30 min. The syringes were then shaken vigorously for 20 times in 7 seconds (as per the description test method) and IVV material expelled from the syringes into individual 1.5 ml microfuge tubes (Eppendorf, Hamburg, Germany). An aliquot (200 µl) of each sample was then loaded onto a 96-well microtiter UV microplate (Thermo Fisher Scientific, Wilmington, USA); 200 µl of Vaccine Diluent was also added to a well of the assay plate as a background control. The Vaccine Diluent consists of a variety of salts, including sodium chloride, monobasic sodium phosphate, dibasic sodium phosphate, monobasic potassium phosphate, potassium chloride and calcium chloride.[32]

A TECAN Infinite® M200 microplate reader and Magellan Software v7.0 (Tecan Group Ltd, Männedorf, Switzerland) were used to perform UV-visible absorbance readings of the samples over the wavelength range of 250 to 400 nm. Final absorbance vs. wavelength profiles of the IVV samples were generated by subtraction of the background control data (Vaccine Diluent) from the sample data.

Statistical analysis
Statistical analysis of the data generated from DLS and UV-visible absorbance spectroscopy analysis was performed in GraphPad Prism v6.04 (GraphPad Software, Inc., California). One-way ANOVA with a post-hoc Tukey's multiple comparisons test was applied to compare the mean data sets between each of the 5 different lots of IVV. Probability values (P) of less than 0.05 were considered as statistically significant.

Conclusion

Many protein-based pharmaceuticals exhibit a wide range of agglomeration phenomena. The split virion influenza vaccine utilized as the model therapeutic agent in the current study is defined in the EP as an aqueous suspension comprising strains of influenza virus. While individual methods have been utilized to examine purified protein formulations, no single technique is capable of evaluating complex formulations such as the split IVV, wherein pleomorphic and heterogeneous protein/lipid complexes and agglomerates may be present.

This investigation revealed the usefulness and suitability of various methods in evaluating the sedimentation and agglomeration characteristics inherent to a complex biopharmaceutical product such as influenza vaccine. The description test demonstrated that the stability criteria for parenteral suspensions based on pharmacopoeial standards were met in terms of product appearance and the ability to resuspend upon agitation. Imaging using correlative microscopy which combines both light and electron microscopy techniques, verified the presence of typical influenza structures as well as agglomerated material. Furthermore, DLS and UV-visible absorbance spectroscopy were useful

orthogonal methods in providing consistent and reproducible data that correlated well with the ODT results. The ODT assay proved to be a simple, practical, rapid and valuable method in quantifying the level of agglomeration.

Therefore, the use of several complementary methods described in this investigation has demonstrated a pragmatic approach toward adequately addressing pharmacopoeial and regulatory requirements for IVV, in terms of product appearance and agglomeration. Further work would be required to ascertain whether the use of multiple orthogonal methods as applied in this study, can be correlated to other vaccine attributes, including potency, virus splitting profile, sterility and/or total protein.

Disclosure of Potential Conflicts of Interest

No potential conflicts of interest were disclosed.

References

1. WHO. Influenza (seasonal) fact sheet no. 211. http://www.who.int/mediacentre/factsheets/fs211/en/index.html (2009); Accessed on 10th January 2014
2. Bernstein DI, Zahradnik JM, DeAngelis CJ, Cherry JD. Clinical reactions and serological responses after vaccination with whole-virus or split-virus influenza vaccines in children agred 6 to 36 months. Pediatrics 1982; 69:404-8; PMID:7070886
3. Gross PA, Ennis FA, Gaerlan PF, Denson LJ, Denning CR, Schiffman D. A controlled double-blind comparison of reactogenicity, immunogenicity, and protective efficacy of whole-virus and split-product influenza vaccines in children. J Infect Dis 1977; 136:623-32; PMID:335000; http://dx.doi.org/10.1093/infdis/136.5.623
4. Furminger IGS. Vaccine production. In: Nicholson KG, Webster RG, Hay AJ, eds. Textbook of Influenza. Oxford: Blackwell Science, 1998:324-32
5. Hoyle L, Barker SM. Fractionation of the influenza virus with the object of producing subunit vaccine. Postgrad Med J 1973; 49:193-94; PMID:4802482; http://dx.doi.org/10.1136/pgmj.49.569.193
6. Scheid A, Caliguiri LA, Compans RW, Choppin PW. Isolation of paramyxovirus glycoproteins. Association of both hemagglutinating and neuraminidase activities with the larger SV5 glycoprotein. Virology 1972; 50:640-52; PMID:4118317; http://dx.doi.org/10.1016/0042-6822(72)90418-7
7. EP. Monographs on vaccines for human use – influenza vaccine (split virion, inactivated). Monograph no. 01/2008:0158. European Pharmacopoeia (8th Edn) 2013; 1:861-63
8. Pharmaceutical suspensions. In: Mahato RI, ed. Pharmaceutical Dosage Forms and Drug Delivery. Boca Raton, FL, USA: CRC Press, 2007:123-33
9. EP. Monographs on dosage forms – Parenteral preparations injections. European Pharmacopoeia (8th Edn) 2013; 1:796-97
10. FDA. Guidance for industry – immunogenicity assessment for therapeutic protein products. Food Drug Admin 2014:1-36
11. EMA. Guideline on influenza vaccines – quality module. Eur Med Agency Sci Med Health 2014:1-34
12. Webster RG, Granoff A. Encyclopedia of virology. In: Palese P, Garciá-Sastre A, eds. Influenza Viruses: Molecular Biology. San Diego, CA: Academic Press, 1994

13. Mie G. Beiträge zur Optik trüber Medien, speziell kolloidaler Metallösungen. Annalen der Physik 1908; 330:377-445; http://dx.doi.org/10.1002/andp.19083300302
14. Finke JM, Roy M, Zimm BH, Jennings PA. Aggregation events occur prior to stable intermediate formation during refolding of interleukin 1beta. Biochemistry 2000; 39:575-83; PMID:10642182; http://dx.doi.org/10.1021/bi991518m
15. Lomakin A, Teplow DB, Kirschner DA, Benedek GB. Kinetic theory of fibrillogenesis of amyloid beta-protein. Proc Natl Acad Sci USA 1997; 94:7942-47; PMID:9223292; http://dx.doi.org/10.1073/pnas.94.15.7942
16. Gupta P, Hall CK, Voegler AC. Effect of denaturant and protein concentrations upon protein refolding and aggregation: a simple lattice model. Protein Sci 1998; 7:2642-52; PMID:9865959; http://dx.doi.org/10.1002/pro.5560071218
17. Aitken A, Learmonth MP. Protein determination by UV absorption. In: Walker JM, ed. The Protein Protocols Handbook. Totowa, NJ, USA: Humana Press Inc., 2002:3-6
18. Wang W, Wang YJ, Wang DQ. Dual effects of Tween 80 on protein stability. Int J Pharm 2008; 347:31-38; PMID:17692480; http://dx.doi.org/10.1016/j.ijpharm.2007.06.042
19. Philo JS. A critical review of methods for size characterization of non-particulate protein aggregates. Curr Pharm Biotechnol 2009; 10:359-72; PMID:19519411; http://dx.doi.org/10.2174/138920109788488815
20. Striegel AM. Thermodynamic equilibrium of the solute distribution in size-exclusion chromatography. J Chromatogr 2004; 1033:241-45; http://dx.doi.org/10.1016/j.chroma.2004.01.040
21. Calvin GJ. The Field-Flow Fractionation Family: Underlying Principles. New York, NY: John Wiley & Sons, 2000
22. Laue TM, Stafford WF. Modern applications of analytical ultracentrifugation. Annu Rev Biophys Biomol Struct 1999; 28:75-100; PMID:10410796; http://dx.doi.org/10.1146/annurev.biophys.28.1.75
23. Reschiglian P, Zattoni A, Roda B, Michelini E, Roda A. Field-flow fractionation and biotechnology. Trends Biotechnol 2005; 23:475-83; PMID:16061297; http://dx.doi.org/10.1016/j.tibtech.2005.07.008
24. Schuster TM, Toedt JM. New revolutions in the evolution of analytical ultracentrifugation. Curr Opin Struct

Biol 1996; 6:650-58; PMID:8913688; http://dx.doi.org/10.1016/S0959-440X(96)80032-7
25. Pekar AH, Frank BH. Conformation of proinsulin. A comparison of insulin and proinsulin self-association at neutral pH. Biochemistry 1972; 11:4013-16; PMID:4673642; http://dx.doi.org/10.1021/bi00772a001
26. Brems DN, Alter LA, Beckage MJ, Chance RE, DiMarchi RD, Green LK, Long HB, Pekar AH, Shields JE, Frank BH. Altering the association properties of insulin by amino acid replacement. Protein Eng 1992; 5:527-33; PMID:1438163; http://dx.doi.org/10.1093/protein/5.6.527
27. Giddings JC. Field-flow fractionation: analysis of macromolecular, colloidal, and particulate materials. Science 1993; 260:1456-65; PMID:8502990; http://dx.doi.org/10.1126/science.8502990
28. Wahlund KG, Litzen A. Application of an asymmetrical flow field-flow fractionation channel to the separation and characterization of proteins, plasmids, plasmid fragments, polysaccharides and unicellular algae. J Chromatogr 1989; 461:73-87; PMID:2708482; http://dx.doi.org/10.1016/S0021-9673(00)94276-6
29. Liu MK, Li P, Giddings JC. Rapid protein separation and diffusion-coefficient measurement by frit inlet flow field-flow fractionation. Protein Sci 1993; 2:1520-31; PMID:8401236; http://dx.doi.org/10.1002/pro.5560020917
30. Nobbmann U, Connah M, Fish B, Varley P, Gee C. Dynamic light scattering as a relative tool for assessing the molecular integrity and stability of monoclonal antibodies. Biotechnol Genet Eng Rev 2007; 24:117-28; PMID:18059629; http://dx.doi.org/10.1080/02648725.2007.10648095
31. Malvern. Dynamic light scattering: common terms defined. Malvern Instruments Limited 2011:1-6
32. bioCSL. Fluvax® vaccine SH 2014 Product Information. http://www.biocsl.com.au/docs/314/677/20130930_SH2014%20Fluvax%20vaccine%20PI_clean_JT_T_dated.pdf (October 2013); Accessed on 29th December 2014
33. Hayat MA, Miller SE. Negative Staining. New York: McGraw-Hill, 1990
34. Esfandiary R, Middaugh CR. Ultraviolet absorption spectroscopy. In: Mahler H-C, Jiskoot W, eds. Analysis of aggregates and particles in protein pharmaceuticals. Hoboken, NJ, USA: John Wiley & Sons, Inc., 2012:171-200